ORIGINAL PAPER

Instability of roll nonlinear system with structural clearance in rolling process

Jin-xing Cui[1] · Yan Peng[1] · Jin Wang[1]

Abstract

The vibration instability of the nonlinear dynamic system of the rolls considering the structural clearance was theoretically investigated, which is caused by the roll assembly accuracy deviation in the hot rolling process. Firstly, the dynamic rolling force model was established based on the Целиков model under the influence of the roll grinding deviation and the stability of the deformation zone. Further, the horizontal and vertical direction coupling dynamic model of the work roll was established considering the structural clearance between the roll and mill frame. Then, the nonlinear dynamic equation was solved by the Runge–Kutta method. The simulation results show that the dynamic system presents the nonlinear vibration characteristics, which shows that the instability of the system is a slowly varying response process with the characteristics of self-excited vibration and forced vibration. Finally, the comparison results show the consistency between the simulation and the test.

Abbreviations

a_1	Horizontal vibration coefficient	h_0	Inlet thickness of rolled piece (m)
a_2	Vertical vibration coefficient	h_{10}	Designed outlet thickness of rolled piece (m)
B	Strip width (m)		
c, c_i $(i = 1,2)$	Horizontal damping coefficient (N s m^{-1})	h_1	Outlet dynamic thickness of rolled piece (m)
c_3, c_4	Vertical damping coefficient (N s m^{-1})	h_n	Thickness of neutral panel strip (m)
c_5	Rolling interface contact damping coefficient (N s m^{-1})	h_x	Thickness of strip in deformation zone (m)
c_{s1}, c_{s2}	Vertical damping coefficient between roll and frame (kN s m^{-1})	Δh	Strip reduction (m)
		k	Shear strength of material (MPa)
e, e_i $(i = 1,2)$	Roll grinding deviation (m)	$k_i (i = 1, 2)$	Horizontal stiffness of work roll (kN m^{-1})
e_0	Assembly clearance (m)	k_3, k_4	Vertical stiffness of upper work roll (kN m^{-1})
f_c, f_{ci} $(i = 1,2)$	Nonlinear horizontal damping (kN s m^{-1})	k_5	Contact stiffness of rolling interface (kN m^{-1})
$f_k, f_{ki} (i = 1, 2)$	Nonlinear horizontal stiffness (kN m^{-1})	$k_{si} (i = 1, 2)$	Nonlinear horizontal stiffness (kN m^{-1})
h	Thickness of microelement (m)	K_x	Roll horizontal load parameter (N)
		K_y	Roll vertical load parameter (N)
		l_c	Contact arc length (m)
		$m, m_i (i = 1, 2)$	Mass of work rolls (kg)
		P	Dynamic rolling force (N)
		P_0	Stable production rolling force (N)
		p	Pressure of microelement (MPa)

✉ Yan Peng
   pengy516@163.com; pengyan@ysu.edu.cn

1   National Engineering Research Center for Equipment and Technology of Cold Rolled Strip, School of Mechanical Engineering, Yanshan University, Qinhuangdao 066004, Hebei, China

$P_{x0}, P_{x0i}(i = 1, 2)$	Horizontal rolling force in stable production (N)
$P_{y0}, P_{y0i}(i = 1, 2)$	Vertical rolling force in stable production (N)
ΔP	Fluctuation of rolling force (N)
$\Delta P_x, \Delta P_{xi}(i = 1, 2)$	Fluctuation of rolling force horizontal component (N)
$\Delta P_y, \Delta P_{yi}(i = 1, 2)$	Fluctuation of rolling force vertical component (N)
$\overline{p}$	Average unit rolling pressure (MPa)
R	Ideal work roll radius (m)
R_e	Roll radius deviation (m)
R_d	Dynamic roll radius (m)
T	Finish rolling temperature (°C)
t	Time variable (s)
v	Rolling speed (m s^{-1})
$x, x_i(i = 1, 2)$	Horizontal displacement of work roll (m)
$\dot{x}, \dot{x}_i(i = 1, 2)$	Horizontal speed of work roll (m s^{-1})
$\ddot{x}, \ddot{x}_i(i = 1, 2)$	Horizontal acceleration of work roll (m s^{-2})
$y, y_i(i = 1, 2)$	Vertical displacement of work roll (m)
$\dot{y}, \dot{y}_i(i = 1, 2)$	Vertical speed of work roll (m s^{-1})
$\ddot{y}, \ddot{y}_i(i = 1, 2)$	Vertical acceleration of work roll (m s^{-2})
δ	Rolling influence coefficient
ϕ	Included angle in rolling interface (°)
γ_d	Dynamic neutral angle (°)
μ	Friction coefficient (m)
ζ	Rolling interface stability coefficient
τ_f	Front tension stress (MPa)
τ_b	Back tension stress (MPa)
τ_s	Shear stress of microelement (MPa)
τ_x	Tension stress in deformation zone (MPa)
ω	Angular speed of work roll (m)
ξ_0	Influence coefficient of back tension
ξ_1	Influence coefficient of front tension

1 Introduction

The vibration control plays an important role in the strip production efficiency and quality. There are many factors affecting the rolling stability, such as the material grade, the hydraulic system accuracy, the strip tension deviation, and the equipment failure [1, 2]. These factors make the rolling mill exhibit different dynamic states, which affect the energy conversion in the process of the strip deformation [3–5]. In engineering, the roll grinding accuracy is often ignored by the production engineers due to its

separation from the strip rolling process [6]. Therefore, it is necessary to analyze the influence mechanism of the roll accuracy for the roll system vibration.

To explore the instability mechanism of a roll system, it is necessary to solve the change of the rolling interface process parameters under the dynamic rolling process. Gao et al. [7] and Zhang et al. [8] established dynamic rolling process parameters in combination with different production problems and further studied the vibration instability of rolling mill dynamic model, which is of great significance for the engineering application. The corresponding rolling process parameter model has been widely studied considering the influence of roll motion on the rolling deformation parameters and the dynamic change of the roll gap [9–14]. The friction coefficient of rolling interface is also an important aspect affecting the rolling force. Liu et al. [15] established the dynamic rolling force model in consideration of the mixed lubrication friction as the boundary lubrication and hydrodynamic lubrication. Lu et al. [16] calculated the lower limit of the friction coefficient in cold tandem rolling mills by developing a new friction model. Wang et al. [17] established the basic model of unsteady hydrodynamic lubrication and analyzed the thickness of unsteady lubricating oil film, pressure stress, and friction stress in the working area of strip rolling with corresponding mathematical and physical methods. In addition, the fluctuation of strip thickness and the dynamic change of the strip tension are also the factors affecting the rolling process [18–21]. However, the existing models all ignore the change of process parameters caused by the roll defects.

The study on the instability factors is one of the key steps to redisplay the vibration characteristics and reveal the vibration mechanism in the rolling process [22–24]. Hu and Ehmann [25, 26] summarized the vibration problems as the triple frequency and quintuple frequency vibration and analyzed the structural differences, and they found that the quintuple frequency is mainly caused by the external excitation of the backup roll. Johnson and Qi [27] established an up-down symmetrical vertical vibration model, explored the influence of roll diameter ratio on the rolling mill chatter, and proposed the control methods by changing the rolling speed, matching the roll diameter ratio, and avoiding the external excitation. Shi et al. [28, 29] comprehensively studied the nonlinear dynamic behavior in the rolling process, which provides a reference for the study of nonlinear vibration. Zang et al. [30, 31] analyzed the vibration test data of a semi-endless rolling (CSP) production line, pointing out that the structural clearance and gear meshing impact are the main manifestations of the rolling mill vibration. However, the vibration instability caused by the coupling effect of the roll grinding accuracy and the rolling deformation stability is still not explicit.

This paper is purposed on the work roll dynamic instability mechanism caused by the roll accuracy deviation and the rolling deformation process instability in the production process. Firstly, the rolling force model under the coupling effect of the roll grinding deviation and the rolling interface stability parameter is established. Secondly, the horizontal and vertical direction vibration dynamic equations are established considering the nonlinear stiffness and damping characteristics of the system caused by roll assembly clearance. The dynamic equation is solved and simulated by the numerical method, and the motion characteristics of roll are further analyzed. The simulation results are consistent with the actual test, which shows the correctness of this study. This paper provides a reference for vibration source identification as well as equipment operation and maintenance in rolling process.

2 Dynamic rolling force model

2.1 Roll grinding deviation

The strip rolling is a complex dynamic process mainly affected by the stability of the rolling interface. In addition to the influence of incoming slab accuracy and microstructure, the dynamic fluctuation caused by the roll accuracy and motion has a great influence on the rolling interface. The error sources in the roll grinding process include poor roll positioning accuracy and grinder chatter [32]. The analysis of roll grinding process in a factory is shown in Fig. 1. Through observation, it is found that the grinder has the problem of poor positioning accuracy, but it is impossible to directly test the roll accuracy and the influence on the rolling process stability. When the rolls in such product condition are used, the rolling force fluctuates periodically with a frequency similar to the roll rotation, and the rolling mill vibrates violently. Therefore, based on the test and analysis, this paper ignores the influence of the electrical system, hydraulic system, and the incoming slab dynamic nonuniformity performance and studies the dynamic instability mechanism of the roll system with clearance influenced by the roll grinding accuracy and dynamic load.

As shown in Fig. 2, the roll gap accuracy deviation occurs due to the grinding process. O' is the grinding axis of the grinder, while O is the working axis in the actual installation position with e. The R_d changes dynamically, which can be expressed as

$$R_d = R - R_e \tag{1}$$

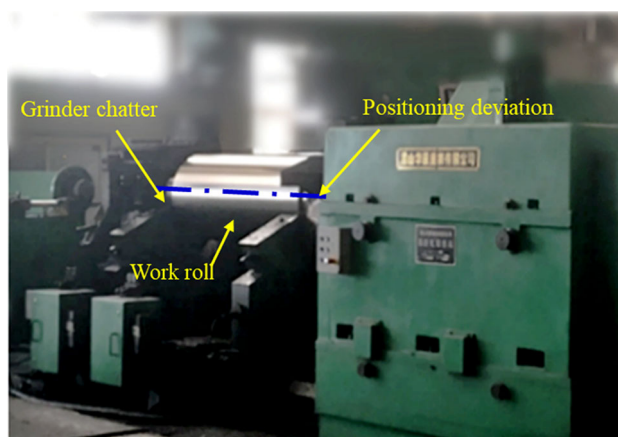The roll radius deviation caused by grinding roll can be expressed as $R_e = e\sin(\omega t)$.

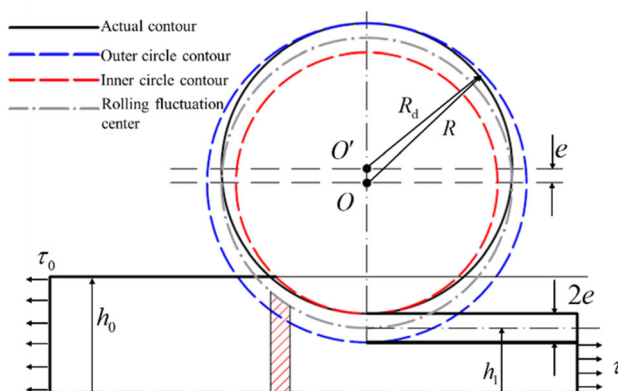
Fig. 1 Grinding process of work roll

Fig. 2 Influence of roll deviation

Assuming that h_0 is uniform and the upper and lower rolls are symmetrical with respect to the rolling centerline, h_1 can be expressed as

$$h_1 = h_{10} + 2(R_d - R) + 2\zeta = h_{10} + 2e\sin(\omega t) + 2\zeta \tag{2}$$

ζ is calculated as

$$\zeta = \sqrt{a_1 \left(\frac{\Delta P_x}{K_x} + a_2 \left(\frac{\Delta P_y}{K_y} \right) \right)} \tag{3}$$

The contact arc length is expressed as

$$l_c = \sqrt{\Delta h(R - e\sin(\omega t))} \tag{4}$$

where $\Delta h = h_0 - h_1$.

2.2 Rolling process parameter model

As shown in Fig. 3, the distribution relationship of internal friction coefficient in rolling deformation zone is considered as mixed friction type. According to Ref. [33], the effects of the external friction, the strip tension and the
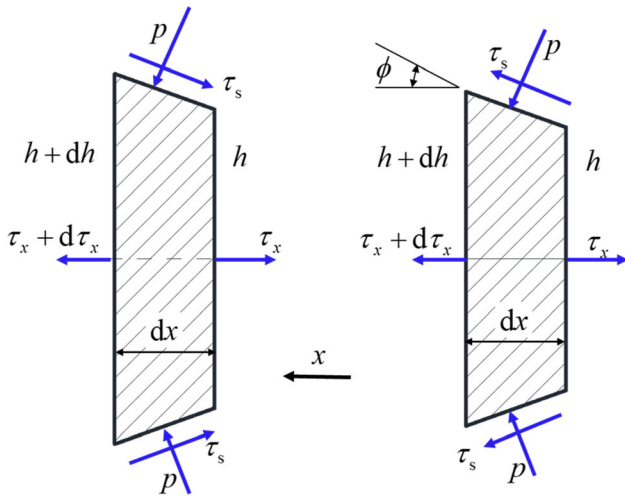
Fig. 3 Deformation stress of strip [35]

rolling deformation strengthening were considered. The average unit rolling pressure can be expressed as

$$\overline{p} = \frac{2k}{\Delta h \delta} \left\{ \int_{h_n}^{h_0} \left[(\xi_0 \delta - 1) \left(\frac{h_0}{h_x} \right)^{\delta} + 1 \right] dh_x + \int_{h_1}^{h_n} \left[(\xi_1 \delta + 1) \left(\frac{h_x}{h_1} \right)^{\delta} - 1 \right] dh_x \right\} \tag{5}$$

where $\delta = \frac{2\mu l_c}{\Delta h}$.

The influence coefficient of strip tension on the rolling force during strip deformation at the rolling interface is expressed as [33]

$$\xi_0 = 1 - \frac{\tau_b}{2k} \tag{6}$$

$$\xi_1 = 1 - \frac{\tau_f}{2k} \tag{7}$$

h_n can be determined by the equal rolling pressure of front sliding zone and rear sliding zone [34], expressed as

$$h_n = \sqrt[2\delta]{\frac{\xi_0}{\xi_1} h_0^{\delta-1} (h_{10} + 2e \sin(\omega t) + \zeta)^{\delta+1}} \tag{8}$$

Based on the Целиков formula [33] considering the strip tension, the dynamic deformation parameters are brought into the dynamic rolling force model. $\overline{p}$ can be expressed as

$$\overline{p} = \frac{1}{\Delta h} \left\{ 2k\xi_0 \frac{h_0}{\delta - 2} \left[\left(\frac{h_0}{h_n} \right)^{\delta-2} - 1 \right] + 2k\xi_1 \frac{h_{10} + 2e \sin(\omega t) + \zeta}{\delta + 2} \left[\left(\frac{h_n}{h_{10} + 2e \sin(\omega t) + \zeta} \right)^{\delta+2} - 1 \right] \right\} \tag{9}$$

The dynamic rolling force is approximately expressed as

$$P = Bl_c\overline{p} = \frac{Bl_c}{\Delta h} \frac{1}{\Delta h} \left\{ 2k\xi_0 \frac{h_0}{\delta - 2} \left[\left(\frac{h_0}{h_n} \right)^{\delta-2} - 1 \right] + 2k\xi_1 \frac{h_{10} + 2e \sin(\omega t) + \zeta}{\delta + 2} \left[\left(\frac{h_n}{h_{10} + 2e \sin(\omega t) + \zeta} \right)^{\delta+2} - 1 \right] \right\} \tag{10}$$

Substituting Eqs. (2)–(9) into Eq. (10), the dynamic rolling force is obtained as

$$P = Bl_c\overline{p} = 2kB \sqrt{\frac{R - e \sin(\omega t)}{h_0 - h_{10} + 2e \sin(\omega t) + \zeta}} \times$$
$$\left\{ \left(1 - \frac{\tau_b}{2k} \right) \frac{h_0}{\delta - 2} \left[\left(\frac{h_0}{2\delta\sqrt{\frac{\xi_0}{\xi_1} h_0^{\delta-1} (h_{10} + 2e \sin(\omega t) + \zeta)^{\delta+1}}} \right)^{\delta-2} - 1 \right] + \xi_1 \frac{h_{10} + 2e \sin(\omega t) + \zeta}{\delta + 2} \left[\left(\frac{2\delta\sqrt{\frac{\xi_0}{\xi_1} h_0^{\delta-1} (h_{10} + 2e \sin(\omega t) + \zeta)^{\delta+1}}}{h_{10} + 2e \sin(\omega t) + \zeta} \right)^{\delta+2} - 1 \right] \right\} \tag{11}$$

As shown in Fig. 3, the rolling interface of the rolling mill is equivalent to a wedge-shaped deformation zone, and ϕ is approximately equal to the neutral angle, then

$$\phi = \gamma_d = \frac{1}{2} \sqrt{\frac{\Delta h}{R_d}} \left(1 - \frac{1}{2\mu} \sqrt{\frac{\Delta h}{R_d}} \right) \tag{12}$$

The horizontal and vertical components of rolling force can be expressed as

$$\begin{cases} P_x = P \tan\phi + \mu P \cot\phi \\ P_y = P \cot\phi + \mu P \tan\phi \end{cases} \tag{13}$$

According to Eq. (11), the rolling force shows time-varying characteristics, which leads to dynamic instability in the rolling process. The fluctuation of rolling force is defined as

$$\begin{cases} \Delta P = P - P_0 \\ \Delta P_x = P_x - P_{x0} \\ \Delta P_y = P_y - P_{y0} \end{cases} \tag{14}$$

According to Refs. [6–9, 11, 15], the vibration energy of roll system comes from the dynamic energy conversion in rolling deformation zone. When the roll diameter changes periodically, the dynamic energy of the rolling interface at instability state flows into the roll dynamic system, resulting in the violent vibration of the rolling mill. Therefore, it is necessary to study the dynamic characteristics of the roll system under the above process conditions.

3 Dynamic model of work roll

The dynamic performance caused by the roll grinding deviation is greatly affected by the gap and the clearance value, especially the horizontal vibration. Therefore, the
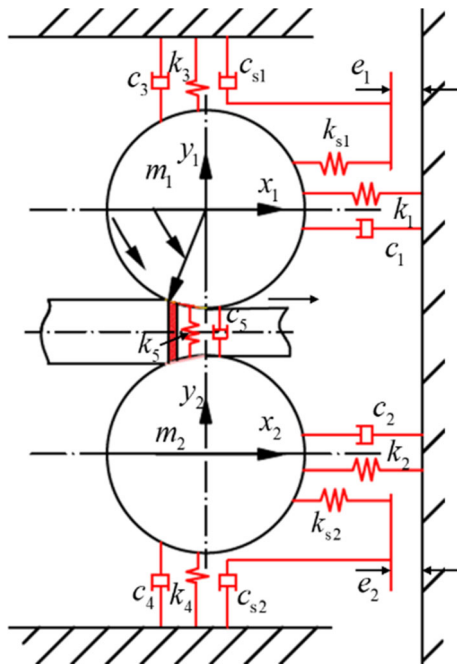
Fig. 4 Coupling dynamic model of roll system

dynamic model was established taking the influence of the structural clearance into account, as shown in Fig. 4. The dynamic differential equation is

$$M\ddot{X} + C\dot{X} + KX = F \tag{15}$$

where $M = \begin{bmatrix} m_1 & 0 & 0 & \\ 0 & m_1 & 0 & 0 \\ 0 & 0 & m_2 & 0 \\ 0 & 0 & 0 & m_{12} \end{bmatrix}$,

$K = \begin{bmatrix} k_1 + k_{s1} & 0 & 0 & 0 \\ 0 & k_3 + k_5 & 0 & -k_5 \\ 0 & 0 & k_2 + k_{s2} & 0 \\ 0 & -k_5 & 0 & k_3 + k_5 \end{bmatrix}$,

$C = \begin{bmatrix} c_1 & 0 & 0 & 0 \\ 0 & c_3 + c_5 + c_{s1} & 0 & -c_5 \\ 0 & 0 & c_2 & 0 \\ 0 & -c_5 & 0 & c_3 + c_5 + c_{s1} \end{bmatrix}$,

$F = \begin{bmatrix} P_{x01} + \Delta P_{x1} \\ P_{y01} + \Delta P_{y1} \\ P_{x02} + \Delta P_{x2} \\ P_{y02} + \Delta P_{y2} \end{bmatrix}$, and $X = \begin{bmatrix} x - x_1 \\ y - y_1 \\ x - x_2 \\ y - y_2 \end{bmatrix}$.

The structural stiffness and damping characteristics are piecewise nonlinearly affected by the horizontal displacement of the work roll. The piecewise elastic force and damping force caused by the clearance can be expressed as

$$f_{ki} = \begin{cases} k_i x_i & x_i < e_i \\ k_i x_i + k_{si}(x_i - e_i) & x_i \geq e_i \end{cases} \quad (i = 1, 2) \tag{16}$$

$$f_{ci} = \begin{cases} c_3 \dot{y} & x_i < e_i \\ (c_3 + c_s)\dot{y} & x_i \geq e_i \end{cases} \quad (i = 1, 2) \tag{17}$$

Equation (15) is simplified as

$$\begin{cases} \ddot{x}_1 + \dfrac{c_1}{m_1}\dot{x}_1 + \dfrac{f_{k1}}{m_1} = \dfrac{\Delta P_{x1}}{m_1} \\ \ddot{y}_1 + \dfrac{f_{c1}}{m_1} - \dfrac{c_5}{m_1}\dot{y}_2 + \dfrac{(k_3 + k_5)}{m_1}y_1 - \dfrac{k_5}{m_1}y_2 = \dfrac{\Delta P_{y2}}{m_1} \\ \ddot{x}_2 + \dfrac{c_2}{m_2}\dot{x}_2 + \dfrac{f_{k2}}{m_2} = \dfrac{\Delta P_{x2}}{m_2} \\ \ddot{y}_2 + \dfrac{f_{c2}}{m_2} - \dfrac{c_5}{m_2}\dot{y}_1 + \dfrac{(k_4 + k_5)}{m_2}y_2 - \dfrac{k_5}{m_2}y_1 = \dfrac{\Delta P_{y2}}{m_2} \end{cases} \tag{18}$$

Considering the symmetry of the roll system, the structural parameters have the relationships as

$$\begin{cases} m_1 = m_2 \\ c_1 = c_2, k_1 = k_2 \\ c_3 = c_4, k_3 = k_4 \\ f_{c1} = f_{c2}, f_{k1} = f_{k2} \end{cases} \tag{19}$$

The system can be simplified to a two degree of freedom system, expressed as

$$\begin{cases} \ddot{x} + \dfrac{c}{m}\dot{x} + \dfrac{f_k}{m} = \dfrac{\Delta P_x}{m} \\ \ddot{y} + \dfrac{f_c}{m} + \dfrac{(k_3 + k_5)}{m}y = \dfrac{\Delta P_y}{m} \end{cases} \tag{20}$$

4 Simulation and discussion

4.1 Simulation parameters

We tested the vibration problems of the 1780-mm four-high hot tandem mill by measuring the roll system vibration and rolling process parameters. In order to study the formation mechanism of the rolling mill vibration, it is necessary to obtain the main structural dynamic parameters, rolling production process parameters, and equipment operation process parameters. As shown in Fig. 5, the horizontal and vertical vibration acceleration of the work roll bearing pedestal was collected by the sensors. The rolling mill obtains the corresponding rolling parameters through the process parameter data acquisition (PDA) system. Combined with the rolling mill design, the nonlinear dynamic structural parameters are obtained according to Refs. [29–31, 36], as shown in Table 1. Taking the production process of rolling slab steel grade SPAH as the research object, the process parameters of the production process are shown in Table 2.

4.2 Vibration characteristics of work roll

This study comprehensively studies the influence mechanism of roll accuracy and structural clearance under different external conditions. According to Eqs. (12) and (18), the dynamic equation is solved by the Runge–Kutta method [37]. The dynamic characteristics are affected by complex rolling interface energy conversion mechanism and structural state under different grinding accuracies and structural clearances. The roll horizontal vibration without considering the roll grinding deviation and the assembly clearance is shown in Fig. 6. The horizontal displacement of the roll is in a damping attenuation state without rolling interface reduction fluctuation, as shown in Fig. 6a, b. The main attenuation vibration frequency is 53.8 Hz, as shown in Fig. 6c. According to the analysis of the dynamic theory, the damping attenuation frequency is close to the natural frequency of the work roll horizontal dynamic system [38]. Figure 6d shows the Poincare curve, which indicates that the system has quasi-periodicity characteristics. The analysis results show that the roll horizontal motion maintains a stable state without the external excitation of dynamic instability at the rolling interface. Therefore, the horizontal instability is caused by the forced vibration.

Figure 7 shows the vertical vibration of the roll in the zero initial condition, which is characterized by self-excited vibration with slow variation. According to Eq. (9), the rolling force is influenced by the coupled mechanism of the roll dynamic displacement and speed, which forms a stable energy conversion process. As shown in Fig. 7a, the system gradually forms a vibration with stable amplitude. Figure 7b shows that the vertical vibration has slow variation characteristics. Figure 7c, d shows that the natural period of vertical vibration of roll is close to 81.4 Hz, and there is a dynamic change of period with time during the roll movement. The vertical vibration does not have a fixed vibration period due to the coupling dynamic change of the system, resulting in slow variation in the time domain.

The horizontal vibration under the external fluctuation with a frequency of 48 Hz in the zero initial condition is shown in Fig. 8. Figure 8a displays that the negative displacement of the system is large, and there is an obvious impact collision phenomenon. It can be seen that the rolling interface dynamically changes with the force at the rolling interface. The system does not have a fixed period with the motion phase diagram changing dynamically, as shown in Fig. 8b. In Fig. 8c, the roll motion frequencies show the nonlinear vibration characteristic of octave distribution for the collision between the roll and mill frame [21, 31, 38]. It can be seen from the Poincare phase diagram in Fig. 8d that the motion changes dynamically with the rolling deformation process. The horizontal vibration of the rolling mill exhibits time-varying steady vibration under the dynamic fluctuation of the rolling conditions.

The vertical vibration is manifested in the coupling effect of the system self-excited vibration and external excitation, as shown in Fig. 9. Under the dynamic fluctuation frequency of 48 Hz at the rolling interface, there is a
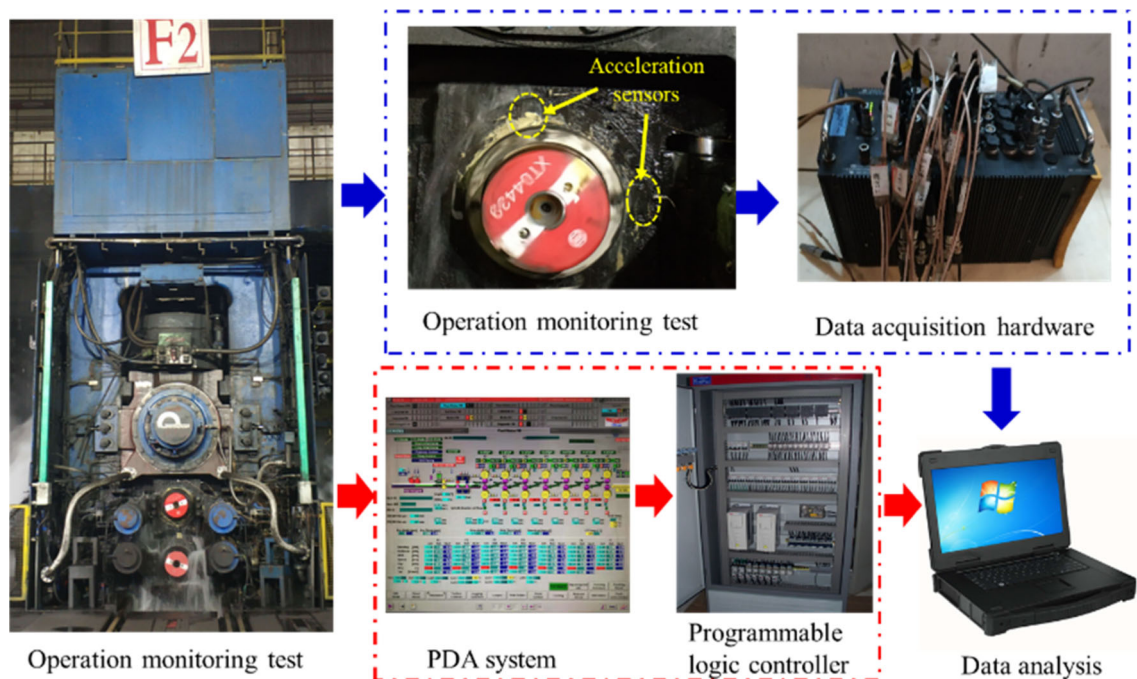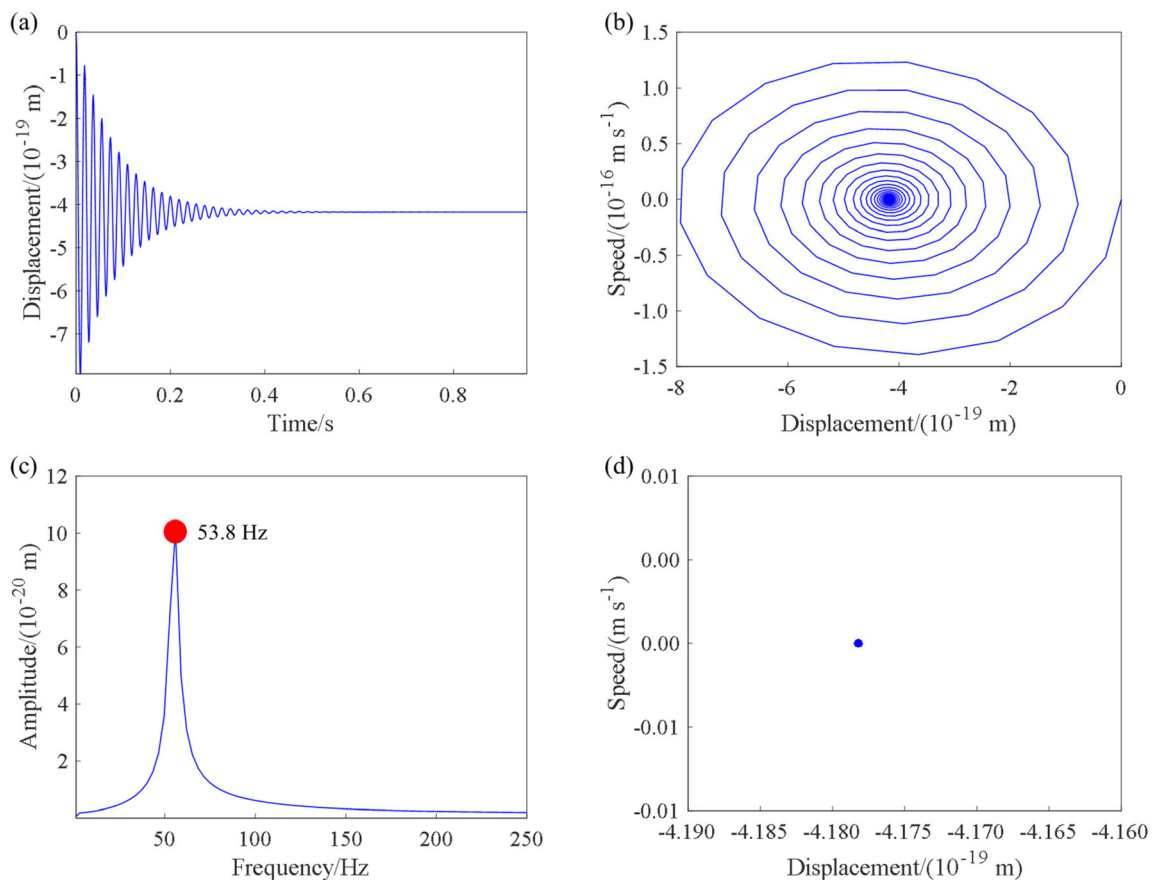

Fig. 5 Data acquisition and processing

Table 1 Structural parameters of F2

m	e_0	e	c_1	c_3	c_5	c_{s1}	k_1	k_3	k_5	k_{s1}	R
18,637	$0\text{–}2 \times 10^{-7}$	$0\text{–}6 \times 10^{-7}$	4.5×10^5	5.7×10^4	7.4×10^4	6.4×10^4	1.2×10^9	7.511×10^{11}	8.2×10^9	3.64×10^{10}	410

Table 2 Rolling parameters of studied strip

Steel grade	B	h_0	h_1	T	k	μ	τ_f	τ_b	v
SAPH	1.25	0.01305	0.0061	920	102	0.27	9.2	5.7	2.4

Fig. 6 Horizontal vibration of work roll ($e = 0$, $e_0 = 0$, $\zeta = 0$). **a** Time domain diagram; **b** phase diagram; **c** frequency domain diagram; **d** Poincare diagram

small vibration displacement of about 1.4×10^{-7} m, while a large displacement occurs at 13.56, 50.98, 85.81, and 93.84 s, as shown in Fig. 9a. Figure 9b indicates that the system forms a stable vibration state under the action of the dynamic mechanism of the rolling interface. Figure 9c shows that the vertical vibration displacement frequency is mainly affected by the characteristics of the excitation frequency of 48.0 Hz and the system natural frequency of 79.9 Hz. The roll vertical system was characterized by the

self-excited and forced vibration phenomenon at the same time. The Poincare phase diagram in Fig. 9d shows that the vertical vibration has no fixed periodicity. The above analysis results show that the vertical direction is excited by the external excitation of the stable frequency state, which presents a slow variation in time domain. According to the model shown in Fig. 5, the vertical motion and horizontal motion are coupled through the system damping. When the dynamic collision occurs between the roll and
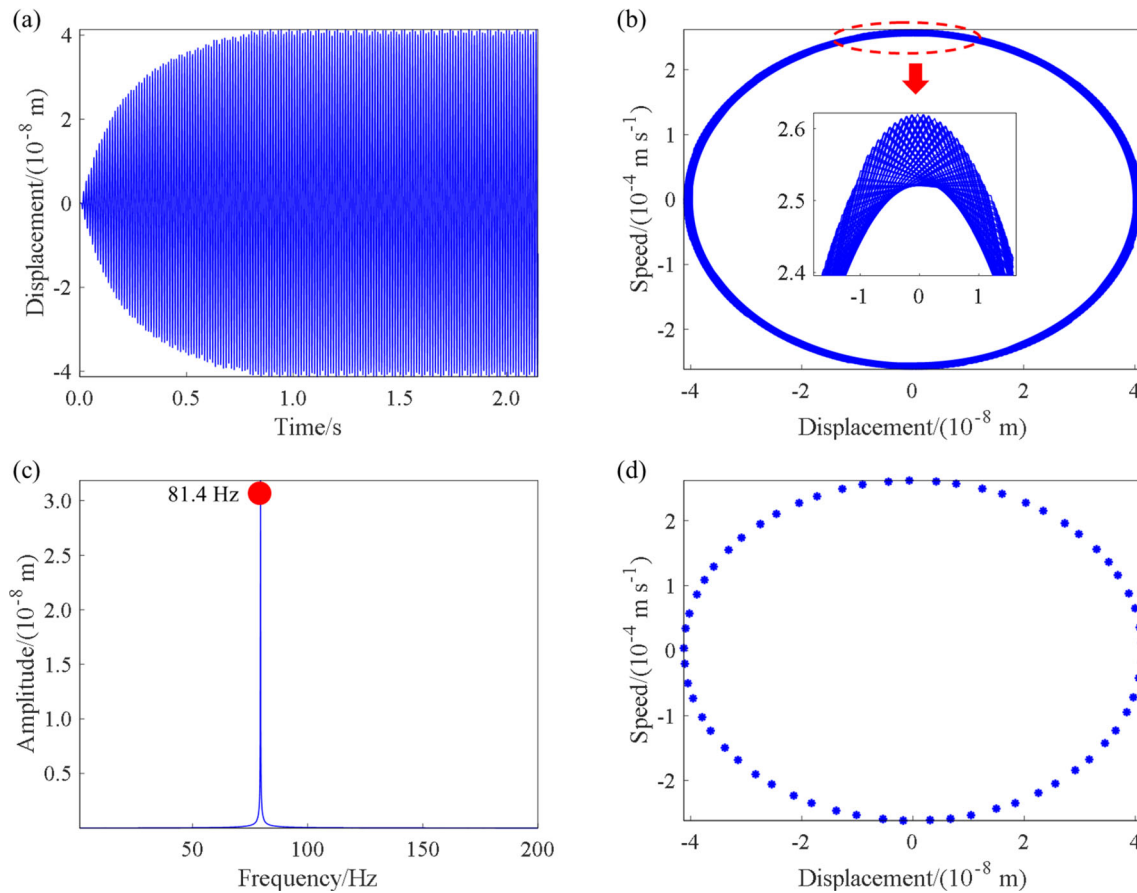
Fig. 7 Vertical vibration of work roll ($e = 0$, $e_0 = 0$, $\zeta = 0$). **a** Time domain diagram; **b** phase diagram; **c** frequency domain diagram; **d** Poincare diagram

the mill frame, the vertical damping may form a negative damping condition [3, 13], and the roll has a large vibration displacement, as shown in the local enlarged view in Fig. 9a.

The following analysis shows the work roll vibration with $e_0 = 3.8 \times 10^{-4}$ m, $e = 1.4 \times 10^{-4}$ m and $\zeta = 8 \times 10^{-5}$, as shown in Fig. 10. There is an obvious cut-top phenomenon in the horizontal vibration problem, indicating that the roll has a dynamic collision with the mill frame in the production process. The period is 1.073 s, which is similar to the rotation period of work roll, as shown in Fig. 10a. It can be seen from the phase diagram (Fig. 10b) that two closed-loop curves between roll speed and displacement present the dynamic change of vibration track. The main vibration frequencies are 1 Hz (low frequency) and 48 Hz, along with other harmonic components of 26, 68, and 86 Hz, as shown in Fig. 10c. These frequency components increase the possibility of harmonic resonance instability. Figure 10d shows that the horizontal vibration has the characteristics of periodic slow change phenomenon under the condition of periodic fluctuation of roll diameter. The above analysis shows that the roll

horizontal vibration is mainly affected by the periodic action of the grinding roll deviation. At the same time, the superposition effect of the vibration is caused by the dynamic change of the rolling interface.

As shown in Fig. 11, the vertical vibration under the condition of dynamic instability of rolling interface is analyzed. Figure 11a shows that the vertical displacement has an approximate period similar to the roll rotation frequency. The displacement peaks in the positive and negative directions are different. The phase diagram in Fig. 11b depicts that the complex motion is caused by the coupling action of the instability strip deformation process and the work roll vibration. The vibration frequencies of the vertical vibration spectrum are 1.0, 48.0, 78.9, and 86.0 Hz, indicating that the system shows the conjoint characteristic of the self-excited vibration and nonlinear impact characteristics. The Poincare phase diagram shows that the system does not have a fixed period, as shown in Fig. 11d. The amplitude and frequency are affected by the horizontal collision between the roll and the mill frame, resulting in an asymmetric movement. The above analysis indicates
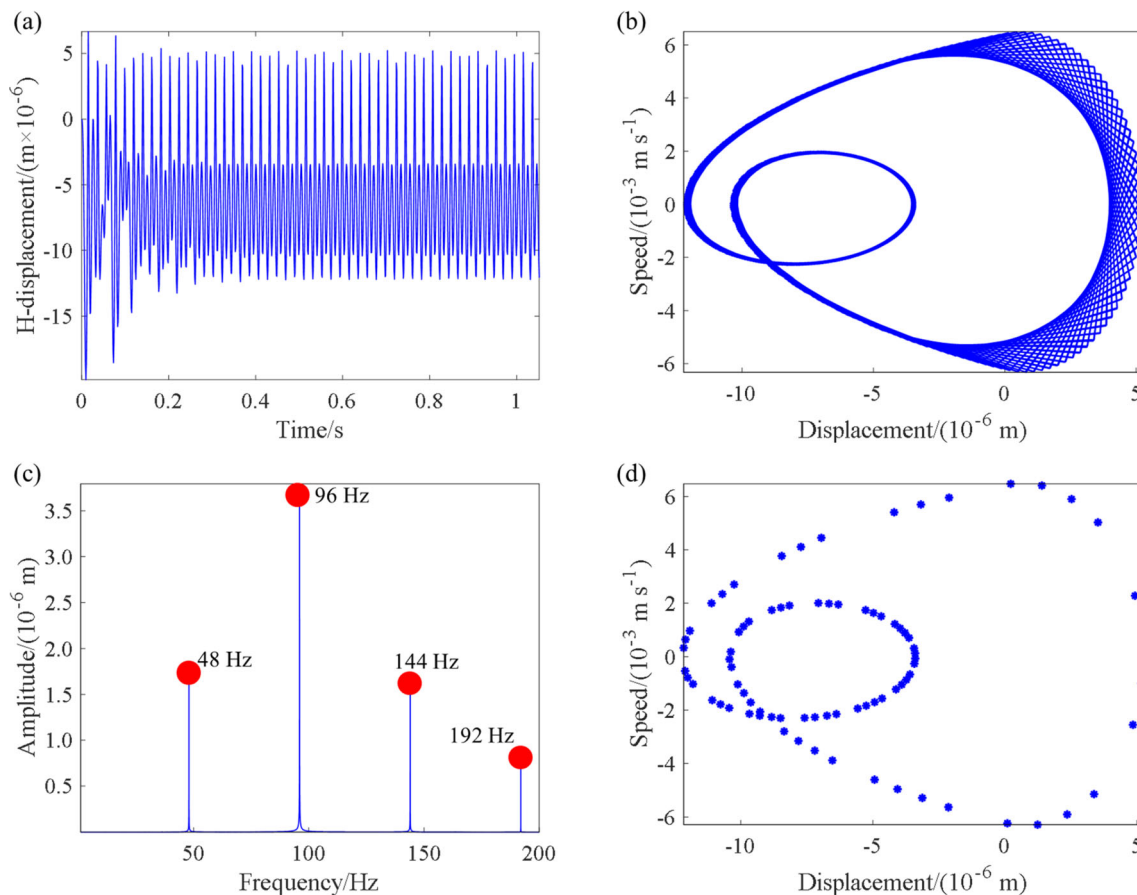
Fig. 8 Horizontal vibration of work roll ($e = 0$, $e_0 = 4 \times 10^{-6}$, $\zeta = 8 \times 10^{-6}$). **a** Time domain diagram; **b** phase diagram; **c** frequency domain diagram; **d** Poincare diagram

that the system is affected by both the roll accuracy and the dynamic fluctuation at the rolling interface.

4.3 Influence factors

The above simulation results indicate that the roll grinding accuracy deviation and the deformation zone instability cause the severe collision in the system. Figure 12 analyzes the influence of the above factors on the vibration displacement. Figure 12a shows that the horizontal vibration increases with the degree of the rolling deformation zone instability and roll deviation. In region A, the grinding roll accuracy has little effect on the vibration amplitude, and thus, the stability of rolling interface is the main factor affecting roll vibration. In particular, the roll shows small horizontal displacement when the grinding roll deviation is less than 4×10^{-5} m. In region B, the horizontal vibration amplitude increases linearly with roll deviation, exhibiting the combined influence of the above factors on the roll dynamic stability. Figure 12b shows the vertical vibration amplitude of the roll system, which increases with the grinding roll deviation and the rolling interface instability.

In region C, the vertical vibration amplitude changes nonlinearly when the rolling interface is stable. In conclusion, the rolling interface stability and roll accuracy are all the key influencing factors of rolling mill vibration instability.

4.4 Result verification

In order to verify the vibration instability in the rolling process, the data of the roll system vibration and the rolling process parameters of the 1.5-mm SPAH slab were tested. Figure 13a shows that under the conditions of the roll grinding deviation of 5×10^{-5} m and the dynamic fluctuation of rolling interface of 5×10^{-5} m, the simulation result of the dynamic rolling force is consistent with the test in the actual rolling process. It can be seen that the roll accuracy deviation and motion instability of the roll are likely to be the reason for the large rolling force deviation. Figure 13b analyzes the dynamic spectrum characteristics of the rolling force. The data acquisition frequency of the PDA system is only 100 Hz, which limits the frequency analysis range only from 0 to 50 Hz. According to the
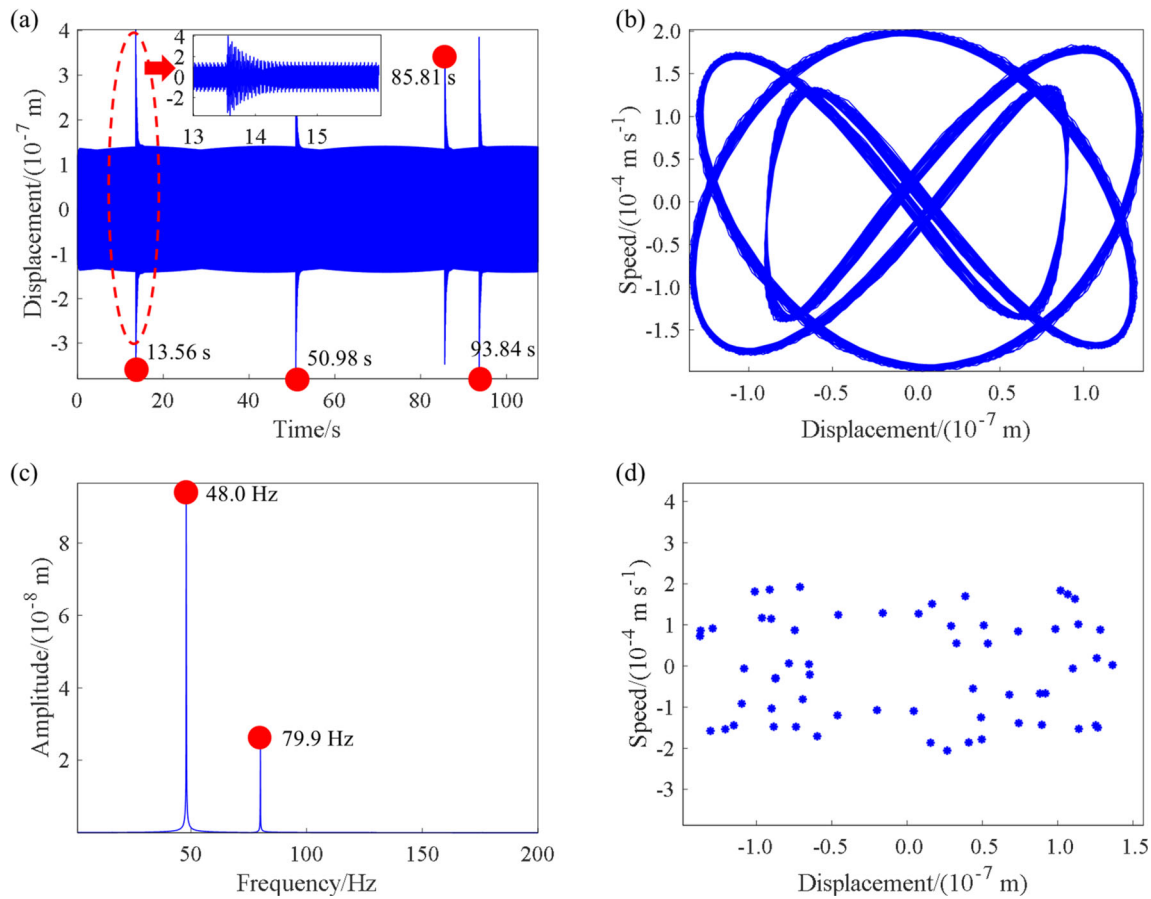
Fig. 9 Vertical vibration of work roll ($e = 0$, $e_0 = 4 \times 10^{-6}$, $\zeta = 1.6 \times 10^{-5}$). **a** Time domain diagram; **b** phase diagram; **c** frequency domain diagram; **d** Poincare diagram

results of fast Fourier transform (FFT), the actual rolling force contains the frequency components of 1 and 49.1 Hz, which is consistent with the results obtained by simulation. In addition, the actual rolling force also contains the frequency components like 16.6 and 33.5 Hz, which is related to the complex dynamic deformation mechanism. The results show that the dynamic rolling force model considering the dynamic rolling interface and the roll grinding deviation can be used as the basis to characterize the instability of rolling mill.

In the rolling process, the displacement is obtained by the secondary integration of the horizontal and vertical accelerations of the work roll, as shown in Fig. 14. Figure 14a shows that the horizontal direction is approximately characterized by periodic impact vibration. The high-frequency vibration occurs in each cycle, which can judge that there is a large systematic impact on the roll. At the same time, the time domain diagram also shows that the positive displacement is inconsistent with the negative displacement. The results indicate that the roll has a dynamic collision with the frame in the horizontal direction. The roll has vibration frequencies of 1.3, 45.7, 21.7,

and 86.0 Hz, as shown in Fig. 14b. The low frequency of 1.3 Hz is similar to the roll rotation frequency, which is consistent with the simulation results. Figure 14c shows the time domain diagram of the vertical vibration, which is similar to the horizontal vibration. During the collision, the vertical vibration amplitudes in the positive and the negative direction are also inconsistent, indicating that the horizontal and vertical vibration are coupled with each other through the dynamic energy conversion at the rolling interface. The vertical frequency distribution diagram shows that the frequencies are basically consistent with the horizontal vibration. Generally speaking, the consistency of the horizontal and vertical motions of the work roll in the actual rolling process is better than the simulation analysis. The reason is that the simulation process ignores the dynamic factors, including the friction change of the rolling interface, the tension change, and the dynamic response of the strip [10–16, 35]. On the whole, the consistency between the measured results and the simulation can show the feasibility of the method constructed in this paper.
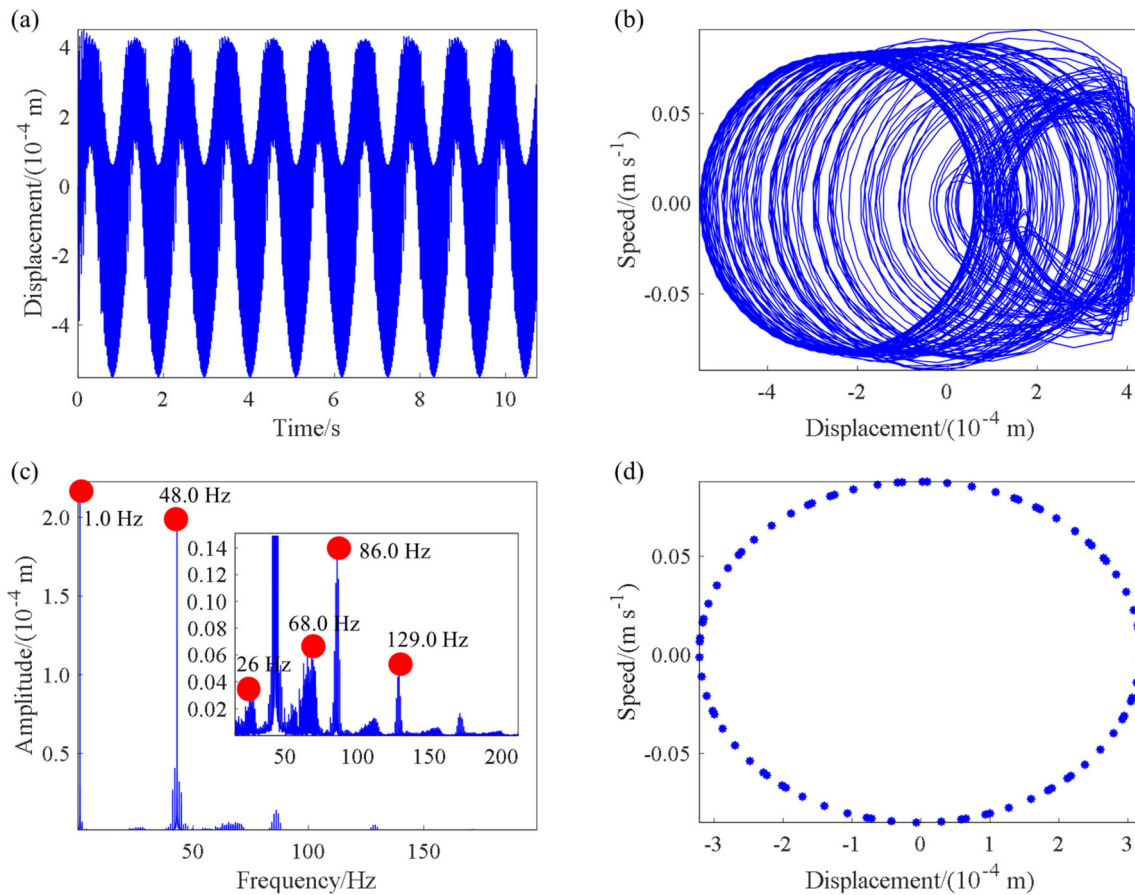
(a)

(b)

(c)

48.0 Hz

1.0 Hz

86.0 Hz

68.0 Hz

129.0 Hz

26 Hz

(d)

Fig. 10 Horizontal vibration of work roll ($e = 1.4 \times 10^{-4}$, $e_0 = 3.8 \times 10^{-4}$, $\zeta = 8 \times 10^{-5}$). **a** Time domain diagram; **b** phase diagram; **c** frequency domain diagram; **d** Poincare diagram

The above analysis and research results show that the roll grinding accuracy dominates the approximate frequency conversion periodic vibration, while the roll dynamic response of the rolling interface and other factors affecting the rolling interface stability further cause the complex dynamic instability characteristics of the rolling mill system. In engineering, by reducing the horizontal clearance, the kinetic energy in the horizontal direction of the roll system can be reduced, and the stability of the rolling interface can be improved. For the roll horizontal and vertical coupling dynamic system with the assembly clearance, the collision between the roll and the mill frame leads to the violent vibration on site. It can be seen that controlling the vibration instability of the rolling mill at this stage must start from the following two ways, ensuring the roll grinding accuracy and the stable energy conversion process at the rolling interface. In addition, the structural mutation characteristics of rolling mill under operation state are controlled to ensure the stability of rolling production by using hydraulic linear [39] and adjusting structural clearance [29–31, 38], which has been verified by experiments. The above analysis shows that focusing on

the accuracy control of roll grinding process and reasonably controlling the equipment assembly accuracy and process design can improve the stability of strip production process as a whole.

5 Conclusions

1. The rolling force has a dynamic fluctuation, which leads to the change of the load on the roll. The simulation results of dynamic rolling force model show that the rolling force is affected by the coupling dynamic factors under the influence of roll deviation and the instability in the strip deformation process.

2. The dynamic model simulation results show that the system with the assembly clearance reveals stable damping attenuation vibration and self-excited vibration characteristics without external excitation. The natural frequencies in the horizontal and vertical directions are about 53 and 80 Hz, respectively. Without considering the roll accuracy error, the roll motion presents the coupling characteristics of self-
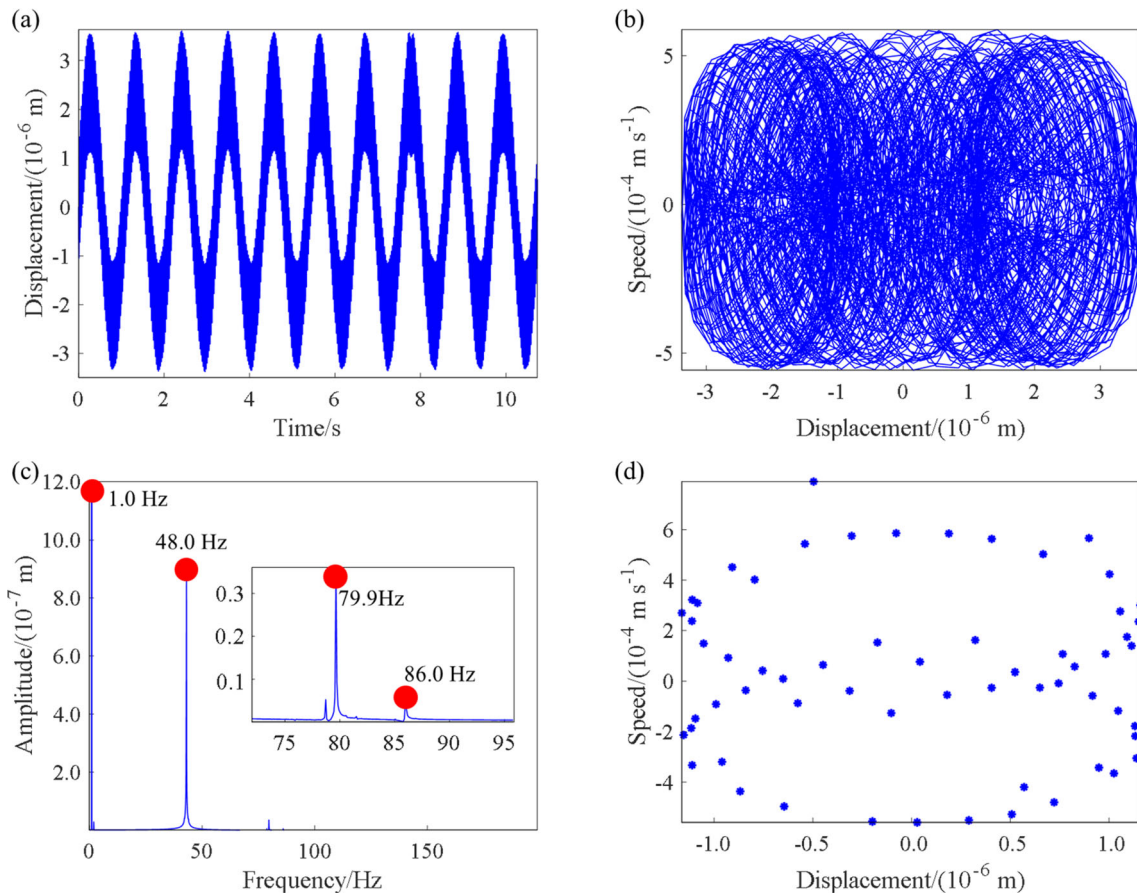
Fig. 11 Vertical vibration of work roll ($e = 1.4 \times 10^{-4}$, $e_0 = 3.8 \times 10^{-4}$, $\zeta = 8 \times 10^{-5}$). **a** Time domain diagram; **b** phase diagram; **c** frequency domain diagram; **d** Poincare diagram
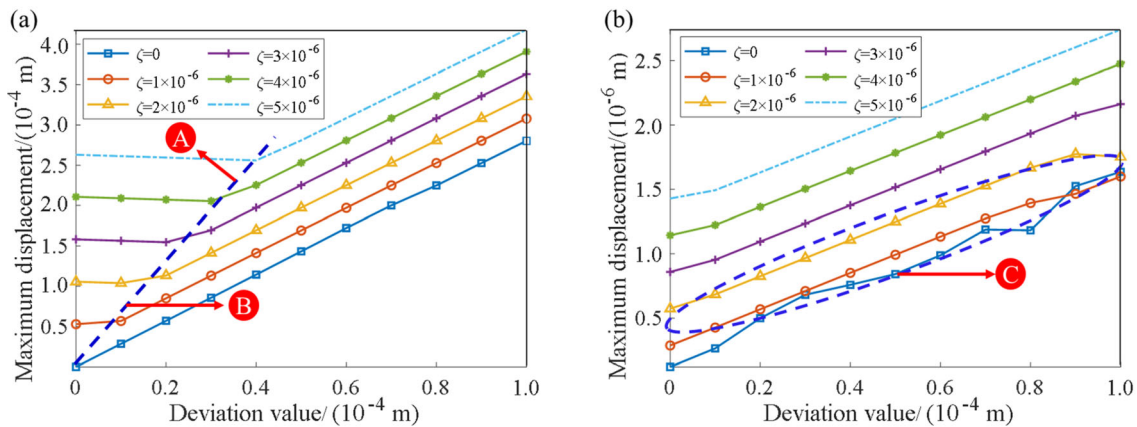

Fig. 12 Maximum displacement amplitude (assembly clearance $e_0 = 3 \times 10^{-4}$). **a** Horizontal direction; **b** vertical direction

excited vibration and forced vibration under the dynamic excitation in the rolling deformation zone. The positive and negative displacements of the roll are not equal, indicating the asymmetry of the roll dynamic system. The roll motion presents the characteristics of slowly varying periodicity under the

coupling dynamic action affected by the roll grinding deviation and the instable dynamic rolling deformation process. The dynamic instability vibration is affected by both the roll accuracy and the dynamic fluctuation in the strip deformation process.
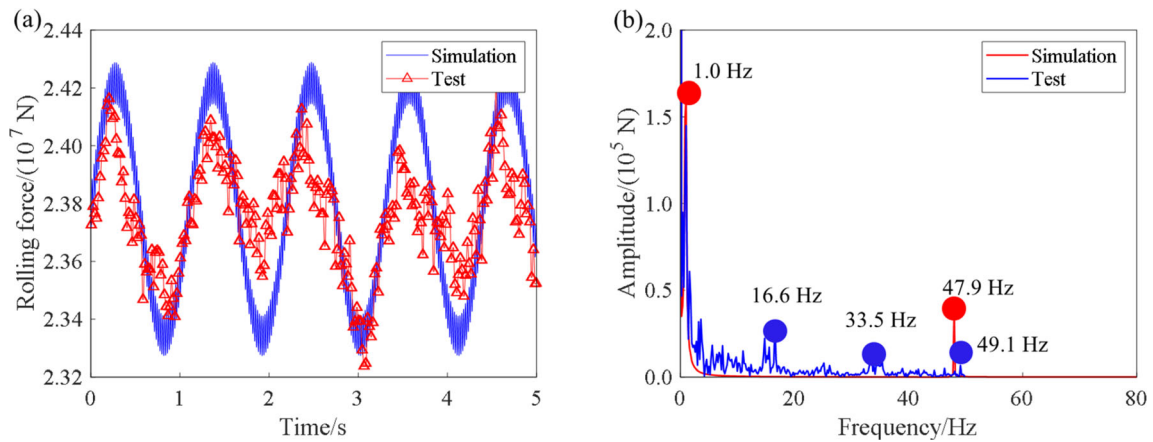
Fig. 13 Comparative analysis of rolling force. **a** Time domain diagram; **b** frequency domain diagram
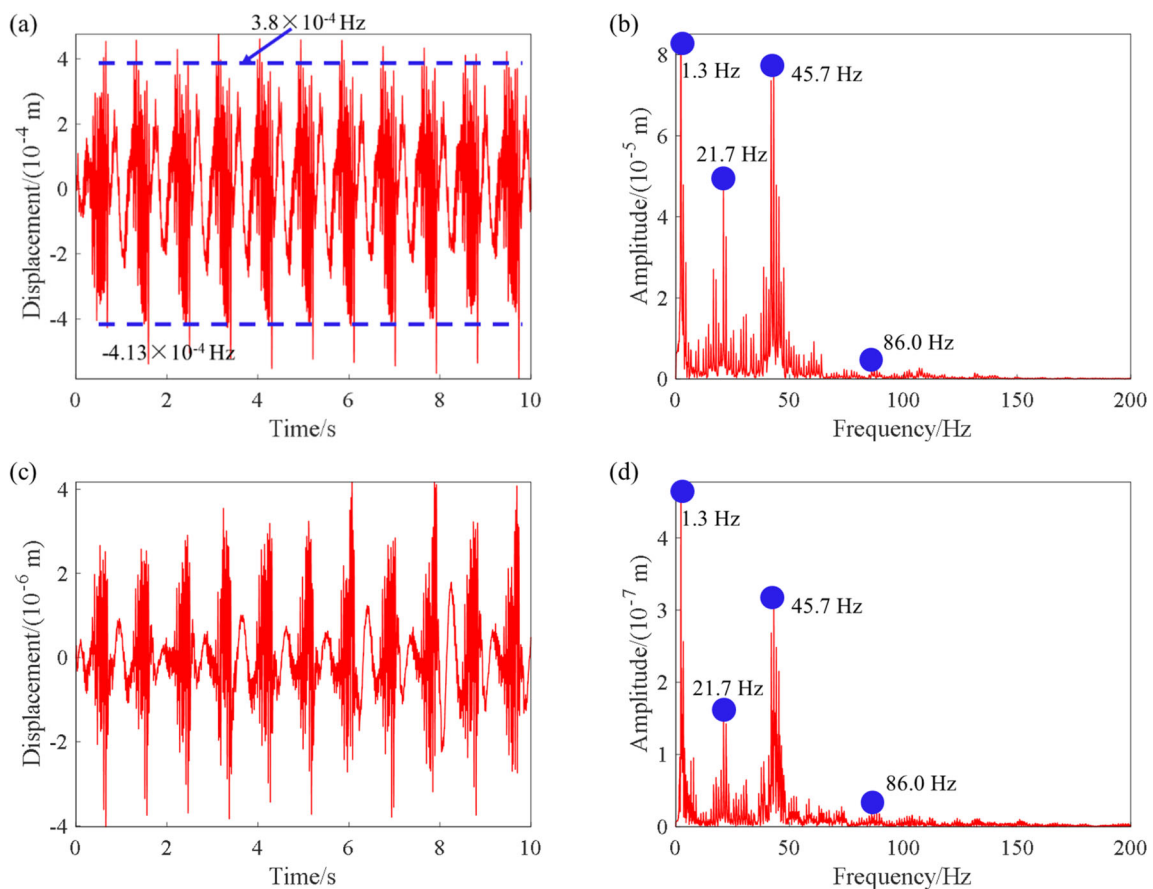

Fig. 14 Analysis of vibration test data of work roll. **a** Time domain diagram of horizontal direction; **b** frequency domain diagram of horizontal direction; **c** time domain diagram of vertical direction; **d** frequency domain diagram of vertical direction

3. The rolling force simulation result is consistent with the actual rolling force. At the same time, the roll motion of the simulation and test results appears asymmetric. The roll vibration becomes more severe with the increase in the horizontal clearance and the roll grinding deviation. This study reveals the dynamic instability characteristics in the rolling process under the conditions of roll grinding accuracy deviation and dynamic instability in the rolling process. This study could provide guidance for the equipment calibration and production process parameter optimization.

References

[1] Z.L. Liu, P. Li, J.H. Jiang, B. Liu, J. Manuf. Process. 64 (2021) 1322–1328.

[2] S.A. Elahi, M.R. Forouzan, Thin-Walled Structures 137 (2019) 19–28.

[3] J. Zhong, H.P. Tang, Journal of Vibration, Measurement & Diagnosis 22 (2002) 1–8.

[4] J.N. Aoh, H.K. Hsu, M.F. Chen, Procedia Manuf. 37 (2019) 410–416.

[5] E. Brusa, L. Lemma, D. Benasciutti, Proc. IMechE Part C: J. Mech. Eng. Sci. 224 (2010) 1645–1654.

[6] S.L. Wu, Y.M. Shao, W.T. Xing, X.C. Jian, Y.L. Yuan, Sci. Technol. Eng. 18 (2018) No. 27, 29–35.

[7] Z.Y. Gao, B. Tian, Y. Liu, L.Y. Zhang, M.L. Liao, J. Iron Steel Res. Int. 28 (2021) 168–180.

[8] M. Zhang, Y. Peng, J.L. Sun, H.R. Li, J. Iron Steel Res. Int. 26 (2019) 953–961.

[9] J.L. Sun, Y. Peng, H.M. Liu, Chin. J. Mech. Eng. 26 (2013) 144–150.

[10] T. Xu, D.X. Hou, Z.N. Sun, D.W. Guo, J. Iron Steel Res. Int. 27 (2020) 517–527.

[11] Z.Y. Gao, Y. Liu, Q.D. Zhang, M.L. Liao, B. Tian, Mech. Syst. Signal Process. 140 (2020) 106692.

[12] A. Heidari, M.R. Forouzan, S. Akbarzadeh, ISIJ Int. 54 (2014) 165–170.

[13] Y. Peng, Y. Zhang, J.L. Sun, Y. Zang, Chin. J. Mech. Eng. 28 (2015) 353–362.

[14] X.C. Sha, D.Z. Li, Y.J. Lan, X.G. Zhang, Y.Y. Li, Steel Res. Int. 75 (2004) 330–338.

[15] S. Liu, H.F. Lu, D.X. Zhao, R.N. Huang, J.L. Jiang, Int. J. Adv. Manuf. Technol. 108 (2020) 369–380.

[16] X. Lu, J. Sun, Z. Wei, G.T. Li, D. Zhang, Tribol. Int. 159 (2021) 106958.

[17] Q.Y. Wang, M. Fang, J. Chen, Y. Zhao, Tribology 33 (2013) 495–500.

[18] W.G. Li, S.B. Tan, J.B. Li, L. Li, J. Northeast. Univ. (Nat. Sci.) 32 (2011) 622–625.

[19] V.R. Khramshin, V.M. Salganik, V.A. Zhilina, I.M. Yachikov, in: Proceedings of 2015 International Conference on Mechanical Engineering, Automation and Control Systems (MEACS), IEEE, Tomsk, Russia, 2015, pp. 1–7. https://doi.org/10.1109/MEACS.2015.7414892.

[20] H.F. Wang, X.G. Ren, Y. Rong, Adv. Mater. Res. 690–693 (2013) 3295–3298.

[21] D.X. Hou, Y. Zhu, H.R. Liu. F. Liu, R.R. Peng, J. Mech. Eng. 49 (2013) No. 14, 45–50.

[22] B.C. Huang, W.J. Ma, J.Y. Wang, Z.Y. Luo, B.H. Chai, Steel Rolling 30 (2013) No. 4, 38–42.

[23] X.C. Liu, Z. Yong, Z.Y. Gao, L.Q. Zeng, Shock and Vibration 2016 (2016) 4025650.

[24] T. Farley, Light Metal Age 64 (2006) 12–14.

[25] P.H. Hu, K.F. Ehmann, Int. J. Mach. Tool. Manuf. 40 (2000) 1–19.

[26] P.H. Hu, K.F. Ehmann, Int. J. Mach. Tool. Manuf. 40 (2000) 21–31.

[27] R.E. Johnson, Q. Qi, Int. J. Mech. Sci. 36 (1994) 617–630.

[28] P.M. Shi, B. Liu, D.X. Hou, Chin. J. Mech. Eng. 45 (2009) 132–139

[29] P.M. Shi, B. Liu, Acta Phys. Sin. 56 (2007) 3678–3682.

[30] Y.T. Wang, Y. Zang, D.P. Wu, Q. Qin, X.B. Fan, Journal of Vibration, Measurement & Diagnosis 29 (2009) 209–213.

[31] X.B. Fan, Y. Zang, D.P. Wu, Y.T. Wang, Y.F. Liao, Z.J. Huang, J. Mech. Eng. 43 (2007) No. 8, 198–201.

[32] Y. Li, Study on roll eccentricity control for flat rolling mill, Northeastern University, Shenyang, China, 2008.

[33] H.D. Cao, Mechanical basis of plastic deformation and rolling principle, China Machine Press, Beijing, China, 1981.

[34] Y.K. Sun, Model and control of cold and hot strip mill, Metallurgical Industry Press, Beijing, China, 2010.

[35] J.X. Cui, Y. Peng, J.L. Sun, B.Y. Li, Int. J. Precis. Eng. Manuf. 22 (2021) 1719–1733.

[36] J.X. Zou, Vibration control of tandem cold rolling mill system, Metallurgical Industry Press, Beijing, China, 1998.

[37] X.M. Shi, Z. Weng, Mathematical physics equation and its MATLAB solution, Tsinghua University Press, Beijing, China, 2011.

[38] H.G. Li, B.C. Wen, J.W. Zhang, Shock and Vibration 8 (2001) 262743.

[39] Y.J. Zheng, G.X. Shen, Y.G. Li, M. Li, H.M. Liu, J. Iron Steel Res. Int. 21 (2014) 837–843.